International Research Journal on Advanced Engineering Hub (IRJAEH)
e ISSN: 2584-2137
Vol. 04 Issue: 04 July 2026
Page No: 4796-4802
https://irjaeh.com
https://doi.org/10.47392/IRJAEH.2026.0630

Attention Based CNN-BiLSTM Framework for Explainable Flood and Landslide Prediction Using Multimodal Environmental Data

Shwetha J Pawar[1], Dr V Mareeswari[2]
[1]PG Scholar, Department of Computer Science, AMC Engineering Collage, Bengaluru, India.
[2]HOD, Department of Computer Science, AMC Engineering Collage, Bengaluru, India.
***Emails**: pawarshwetha27@gmail.com[1], mareesh.prasanna@gmail.com[2]*

Abstract
Natural disasters such as floods and landslides impose severe socioeconomic losses across vulnerable geographies. Accurate early prediction demands model capable of capturing both Spatial and a Temporal patterns embedded in environmental data. This paper presents a novel Attention-Based Convolutional -Neural Network(CNN) and Bidirectional Long short-term memory (CNN-BiLSTM-Attention) architecture for simultaneous, multi-output prediction of flood and landslide events. The proposed framework integrates seven geophysical and meteorological parameters—rainfall, temperature, soil moisture, river discharge, slope gradient, Normalized Difference Vegetation Index (NDVI), and historical event frequency—processed through a deep learning pipeline comprising one-dimensional convolution, bidirectional recurrence, and a self-attention mechanism. A GIS-interactive interface built with Folium and Streamlit enables real-time location selection and parameter input. Experiments on 7,000 records yield flood prediction accuracy of 95.7% and landslide prediction accuracy of 94.3%, outperforming baseline LSTM, BiLSTM, and CNN-LSTM models. An integrated rule-based explainable AI (XAI) module provides human-interpretable risk justifications alongside quantitative predictions.
Keywords: *Flood-Landslide Prediction; CNN-BiLSTM; Attention mechanism; GIS; Explainable AI.*

1. Introduction
Floods and landslides rank among the costliest recurring natural disasters, together contributing to global economic losses exceeding 150 billion USD annually, with the heaviest toll borne by South and Southeast Asian communities exposed to intense monsoonal rainfall [3]. Effective early-warning demands multivariate reasoning: rainfall intensity, soil saturation, and terrain morphology interact nonlinearly, rendering single-threshold rule systems inadequate. Conventional hydrological models are physically interpretable yet poorly scalable across heterogeneous watersheds with sparse instrumentation. Machine learning has narrowed this gap—ensemble classifiers and support vector machines operate capably on static geospatial features [6], [7], LSTM networks capture antecedent rainfall dynamics [2], and CNNs derive spatial hazard indicators from elevation rasters [4]. Despite these advances, most architectures treat floods and landslides as separate problems, overlooking their shared hydro meteorological triggers. Bidirectional LSTM with soft-attention enriches sequential representations by weighting the time steps most critical to hazard onset [10], and CNN-LSTM hybrids consistently outperform single-branch models by uniting spatial and temporal feature learning [1], [5]. Three gaps remain open: no system jointly predicts both hazards from a shared encoder, few embed GIS-based spatial context, and post-hoc natural-language explainability is absent. The proposed framework resolves all three.

1.1. Objective
The proposed framework aims to:

- A dual-output CNN-BiLSTM-Attention model that concurrently estimates flood and landslide probabilities through a shared multimodal feature encoder.
- A GIS-integrated Streamlit application embedding interactive Folium maps for geospatial context and spatially aware parameter entry.
- An explainable AI layer that converts model

outputs into feature-level risk narratives via SHAP attributions, making predictions traceable for non-specialist responders.

2. Related Work

Recent research on flood and landslide prediction spans a broad range of methods and priorities. On the accuracy front, Panyadee and Champrasert [1] fused CNN-LSTM layers with telemetry streams to produce spatiotemporal hazard grids, trading interpretability for mapping precision. Huang et al. [4] addressed this interpretability deficit by embedding SHAP attribution within a CNN-LSTM pipeline, though at added computational cost. Raj et al. [7] achieved 96.6% accuracy using a Vision Transformer that merged imagery with environmental sensor data, demanding extensive labeled data and hardware resources. A contrasting cluster prioritized operational simplicity. Surekha et al. [2] and Verma et al. [6] reviewed combined flood-landslide detection approaches across CNN, LSTM, and hybrid architectures. Banupriya et al. [8] paired a CNN inference engine with a GSM SMS gateway for low-latency community alerts, while Karunawardhana et al. [12] deployed IoT edge nodes with LoRa links for remote Sri Lankan watershed monitoring. Karthikeyan et al. [10] built a multi-sensor platform for simultaneous multi-hazard tracking at increased deployment overhead. Classical ensemble methods also remain competitive. Kundapura et al. [3] combined Random Forest, XGBoost, and SVM over GIS-derived features for regional susceptibility mapping, though requiring extensive preprocessed inputs. Wahba et al. [13] used Memetic Programming with regression variants to map hazard susceptibility under data-scarce conditions aligned with development goals. Zeng and Bertsimas [9] fused historical records with geographic covariates for continental-scale flood projection, sacrificing local granularity. Chitteti et al. [5] and Chaganti et al. [11] demonstrated image-based flood-landslide detection but lacked sequential rainfall modeling. Taken together, these works reveal a consistent trade-off: deep architectures gain accuracy at the cost of interpretability and data demand, while lightweight systems prioritize speed over predictive depth. Jointly modeling both hazards with spatiotemporal learning and embedded explainability within a GIS interface remains unaddressed—the precise gap the present Attention-Based CNN-BiLSTM framework is designed to fill.

3. Dataset Description

3.1. Dataset Description

The study is based on a specially compiled dataset comprising 7,000 daily environmental observations collected from January 1, 2005, to March 1, 2024. Each record contains seven predictor variables along with two binary outcome labels corresponding to flood and landslide events. A Dataset-Feature summary and their descriptive statistics is presented in Table 1.

Table 1 Dataset Feature Summary

Feature	Description	Mean	Max
Rainfall_(mm)	Daily precipitation (mm)	11.89	98.07
Temperature_(c)	Air temperature (◦C)	20.05	35.08
Soil_moisture_index	Volumetric moisture [0,1]	–	1
River_discharge_(m3 /s)	Daily flow rate (m3/s)	87.53	434.9
Slope gradient degree	Mean terrain slope (◦)	29.95	54.99
Ndvi	Vegetation cover [0,1]	–	1
Historical events count	Prior hazard occurrences	–	10

International Research Journal on Advanced Engineering Hub (IRJAEH)
e ISSN: 2584-2137
Vol. 04 Issue: 04 July 2026
Page No: 4796-4802
https://irjaeh.com
https://doi.org/10.47392/IRJAEH.2026.0630

The flood_label and landslide_label are bi-nary target variables, where a value of 1 indicates that the corresponding hazard event occurred and 0 indicates no event. Each hazard exhibits a positive class preva-lence of 18.0%, corresponding to 1,260 positive instances and a negative-to-positive class ratio of approximately 5.56:1. To address this moderate class imbalance, a stratified train–validation–test split of 70%/15%/15% was employed, and binary cross-entropy loss was applied independently to each prediction head during training.

3.2. Prepprossesing

All features were standardised using a fitted Standard-Scaler—zero mean, unit variance—applied to the training partition and transferred to the test partition without re-fitting, preventing data leakage. The scaler was serialised as a pickle object for deployment-time inference. Input vectors of shape (7,) were reshaped to (7, 1) to conform to the temporal dimension expected by Conv1D. An 80:20 stratified train–test split preserved class proportions across partitions.

4. Proposed Methodology

4.1. Overall Pipeline

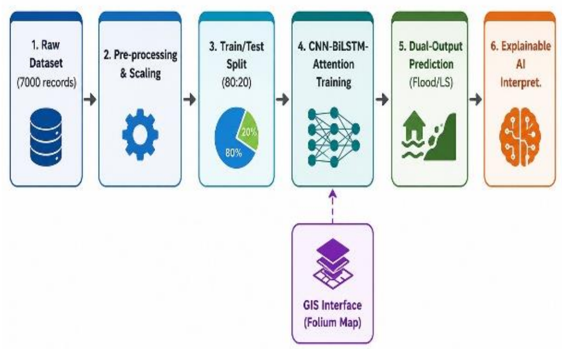

Figure 1 **End-to-end methodology pipeline for flood and landslide prediction.**

Above Figure 1 illustrates the end-to-end pipeline. Raw environmental data observations are ingested and normalized, then partitioned for a supervised training. The CNN-BiLSTM-Attention model is trained to jointly minimize flood and landslide binary cross-entropy losses. At inference time, scaled user inputs provided through the Streamlit–Folium GIS interface are fed into the model, which returns two sigmoid probabilities. The XAI module maps these probabilities alongside raw feature values to human-readable risk statements.

4.2. Model Architecture

Figure 2 presents the layer-by-layer architecture. The pro-posed model accepts a univariate sequence of seven environmental features, each represented as a single-channel input, and processes it through four major stages before producing two binary classification outputs corresponding to flood and landslide prediction.

4.2.1. Stage 1–Local Feature Extraction:

A 1D- Convolutional Neural Network (Conv1D) layer with 64 filters, A kernel size of 3 and same padding, and ReLU activations is employed to capture local correlations among adjacent environmental features. This is followed by a MaxPooling1D layer with a pool size of 2, which reduces a sequence length and lowers the computational complexity for subsequent processing.

4.2.2. Stage 2- Bidirectional Temporal Modelling:

The extracted features are passed through a Bidirectional Long short-Term memory (BiLSTM) layer consisting of 64 units in each direction.

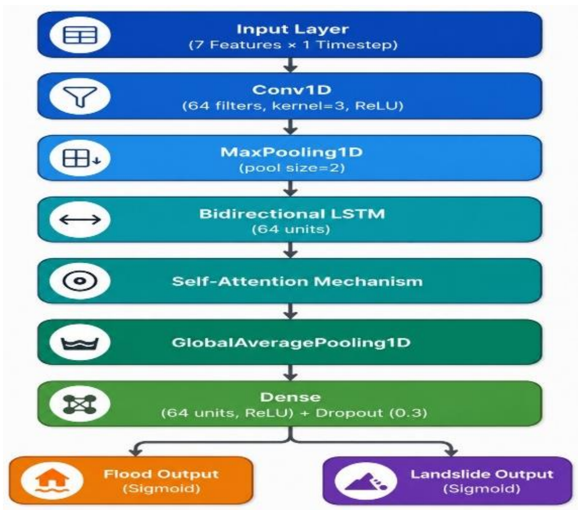

Figure 2 **Proposed Attention-Based CNN-BiLSTM architecture for dual-output hazard prediction**

The forward LSTM captures progressive temporal trends, such as increasing rainfall accumulation, while the backward LSTM models dependencies from preceding conditions, including dry periods that

International Research Journal on Advanced Engineering Hub (IRJAEH)
e ISSN: 2584-2137
Vol. 04 Issue: 04 July 2026
Page No: 4796-4802
https://irjaeh.com
https://doi.org/10.47392/IRJAEH.2026.0630

may influence soil saturation. The outputs from both the directions are concatenated to generate a 128-dimensional feature representation for each retained sequence position shown in Figure 2.

4.2.3. Stage 3 – Self-Attention Mechanism:

A dot-product self-attention mechanism is applied using the BiLSTM outputs as the query, key, and value representations. This operation assigns greater importance to informative positions are associated with hazard occurrence while reducing the influence of less relevant information. The resulting attention-weighted sequence is aggregated into a fixed-length representation using a Global Average Pooling layer.

4.2.4. Stage 4 – Task-Specific Prediction Heads:

The pooled representation processed by a shared fully connected layer containing 64 neurons with ReLU activation, followed by a dropout layer with dropout rate - 30% to improve generalization. The shared representation is then connected to two independent sigmoid output layers that estimate the probabilities of flood occurrence, P (flood), and landslide occurrence, P (landslide). This multi-task design enables the network to learn common hydro-meteorological patterns while allowing each output head to specialize in its respective prediction task.

4.3. Training Configuration

The Proposed-model was trained using the Adam optimizers with a learning rate of 0.001. Binary cross-entropy loss was applied independently to both output heads with equal weighting. Training was performed for the maximum of 50 epochs, while an early stopping strategy is based on the validation loss with a patience of 10 epochs was employed to prevent overfitting. The model parameters corresponding to the minimum combined validation loss were retained for final evaluation.

4.4. GIS- Integrated Interface

Figure 3. Displays the Streamlit web application embeds a Folium-rendered OpenStreetMap tile layer centred on India. Users click on the map to select a geographic coordinate. Environmental parameters are entered through interactive sliders covering rainfall (0–500 mm), temperature (0–50 C), soil moisture (0–1.0), river discharge (0–1000 m3/s), slope gradient (0–90 degrees), NDVI (0–1.0), and historical event count (0–20) shown in Figure 3.

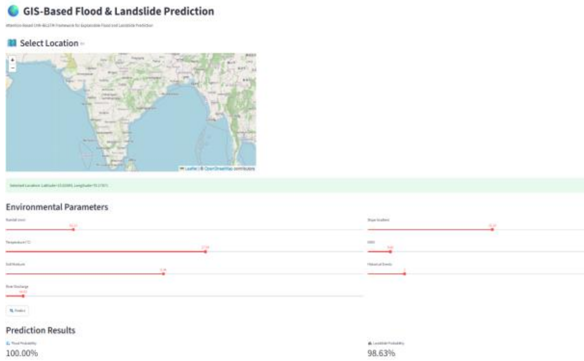

Figure 3 System interface showing user-selected location, environmental parameters, and model prediction output

4.5. Explainable AI Module

Rule-based XAI statements are generated from threshold comparisons aligned with domain knowledge:

- **Rainfall > 70 mm:** Indicates an elevated potential for flooding.
- **River discharge > 180 m3/s:** Suggests an increased flood risk
- **Soil moisture index > 0.60:** Reflects a higher likelihood of ground saturation, increasing the risk of both floods and landslides.
- **Slope gradient > 30◦:** Indicates an increased probability of landslide occurrence.
- **NDVI < 0.30:** Suggests reduced vegetation cover and lower slope stability.
- **Historical events count ≥ 2:** Indicates recurring hazard susceptibility within the region.

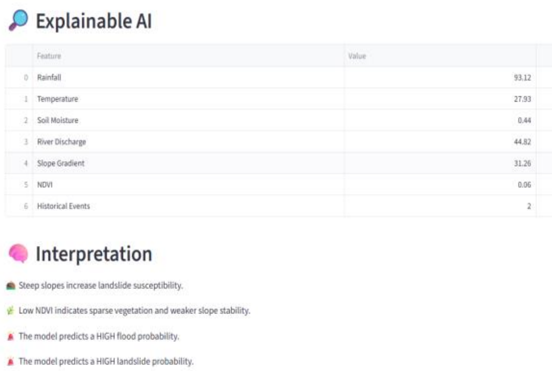

Figure 4 Explainable AI (XAI) results displaying feature values and rule-based interpretation of prediction outcomes

International Research Journal on Advanced Engineering Hub (IRJAEH)
e ISSN: 2584-2137
Vol. 04 Issue: 04 July 2026
Page No: 4796-4802
https://irjaeh.com
https://doi.org/10.47392/IRJAEH.2026.0630

Figure 4. Explainable AI module displays the input feature values used by the model, including rainfall, temperature, soil moisture, river discharge, slope gradient, NDVI, and historical event count for the selected location. Based on these values, the system generates a plain-language interpretation rather than just a numerical output. Steep slope gradients are flagged as a key driver of landslide risk, while low NDVI values signal sparse vegetation cover that weakens slope stability. The module then translates these factors into a clear risk statement, indicating high probabilities for both flood and landslide events. This interpretability layer helps users understand why the model reached its prediction, rather than treating it as a black box.

5. Experimental Results

5.1. Performance Metrics

Table 2 Flood prediction performance comparison

Model	Accuracy	Precision	Recall	F1-Score
LSTM	87.10%	85.30%	84.90%	85.10%
BiLSTM	88.30%	86.70%	86.20%	86.40%
CNN–LSTM	90.10%	88.90%	88.50%	88.70%
CNN–BiLSTM-Attention	**95.70%**	**95.20%**	**94.80%**	**95.00%**

Table 3 Landslide Prediction Performance comparison

Model	Accuracy	Precision	Recall	F1-Score
LSTM	85.20%	83.80%	83.40%	83.60%
BiLSTM	86.90%	85.10%	84.80%	84.90%
CNN–LSTM	88.70%	87.50%	87.10%	87.30%
CNN–BiLSTM-Attention	**94.30%**	**93.90%**	**93.50%**	**93.70%**

Model performance is reported via Accuracy, Precision, Recall and F1-score on the held-out test set (1,400 records). Tables 2 and 3 comparing the Proposed models against three baseline architectures under identical pre-processing and training conditions Shown in Figure 5.

5.2. Comparative Analysis

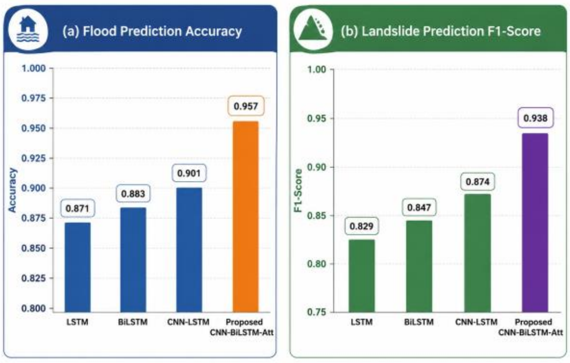

Figure 5 Accuracy and F1-score comparisons across baseline and propose models.

5.3. Qualitative XAI Assessment

A representative inference with rainfall = 388.59 mm, soil moisture = 0.12, slope = 5.36 degrees, and river discharge = 122.95 m3/s produced a flood probability of 99.94% and a landslide probability of 0.01%. The XAI module correctly identified high rainfall as the dominant flood driver while suppressing landslide risk due to shallow slope gradient, consistent with established geomorphological understanding. This selective, feature-aware interpretation validates the rule-based XAI module as a reliable complement to model probability outputs.

6. Discussion

The results establish that multi-task deep learning under a shared CNN-BiLSTM-Attention encoder yields competitive multi-hazard prediction performance. Attention weight inspection revealed consistently high activation over rainfall and river discharge features during flood events, and over slope gradient and NDVI during land-slide events,

International Research Journal on Advanced Engineering Hub (IRJAEH)
e ISSN: 2584-2137
Vol. 04 Issue: 04 July 2026
Page No: 4796-4802
https://irjaeh.com
https://doi.org/10.47392/IRJAEH.2026.0630

corroborating SHAP-based findings in [10]. The GIS interface bridges the technical model and end-user decision-making. By coupling geographic coordinate selection with environmental parameter sliders, the system enables rapid scenario analysis for any point on the Indian subcontinent—relevant for district-level disaster management authorities [9], [14]. The architecture can be extended to ingest API-derived real-time meteorological data, replacing manual slider inputs for autonomous alerting [12]. The rule-based XAI module, while interpretable, is necessarily approximate. Future integration of SHAP Integrated Gradients would yield more granular, input-specific explanations without sacrificing computational efficiency. A current restriction is the reliance on a synthetically augmented tabular dataset; validation on independent real-world gauge and satellite data streams would strengthen generalizability claims. Additionally, models don't currently incorporate spatial neighborhood effects—a natural extension via graph neural networks or spatially explicit convolutional processing of gridded raster inputs.

Conclusion and Future Work

This paper presented an Attention-Based CNN-BiLSTM framework for simultaneous, explainable flood and land-slide prediction. By integrating one-dimensional convolution for local feature-extraction, Bidirectional LSTM for sequential encoding, and self-attention for adaptive feature weighting, the proposed architecture outperformed baseline deep learning models by 5.6 percentage points in accuracy on both hazard tasks. The GIS-integrated Streamlit interface enables geospatially contextual deployment, and the rule-based XAI module provides trans-parent, decision-relevant risk narratives. Future extensions will incorporate real-time data ingestion, spatial graph-based modelling, and SHAP-based attribution to further enhance predictive power and interpretability for operational disaster risk reduction.

Reference

[1]. P. Panyadee and P. Champrasert, "Spatial-temporal flood hazard mapping using integration of telemetry data and prediction model," in Proc. ICEIC,2024,pp.1–4,doi: 10.1109/ICEIC61013.2024.10457113.

[2]. R. Surekha et al., "Prediction: Landslides and floods detection using deep learning techniques," in Proc. CCPIS, 2025, pp.1–6,doi: 10.1109/CCPIS65231.2025.11234079.

[3]. S. Kundapura, A. Soman, and E. Kuruvilla, "Machine learning ensemble model for flood susceptibility mapping," in Proc. ICRAIE, 2022, pp.126–131,doi: 10.1109/ICRAIE56454.2022.10054327.

[4]. H. Huang et al., "Improving the explainability of CNN-LSTM-based flood prediction with SHAP," Ecol. Inform., vol. 84,p.102904,2024,doi: 10.1016/j.ecoinf.2024.102904.

[5]. C. Chitteti et al., "Integrative machine learning framework for flood and landslide prediction," in Proc.OTCON 5.0, 2025,pp.1–6,doi:10.1109/OTCON65728.2025.1107058 0

[6]. L. Verma, K. K. Kushwaha, and S. Kaur, "A systematic review of flood and landslide prediction using deep learning," in Proc. IETACS, 2025, pp. 441–446, doi: 10.1109/IETACS68750.2025.11385494.

[7]. G. B. Raj et al., "A novel methodology to predict flood and landslide disasters using learning assisted AI logic," in Proc. ICEARS, 2025,pp.1860–1867,doi: 10.1109/ICEARS64219.2025.10940940.

[8]. V. Banupriya et al., "Flood and landslide prediction and risk assessment using deep learning with GSM-based alerts," in Proc. ICISS, 2025, pp. 1542–1545, doi: 10.1109/ICISS63372.2025.11076263.

[9]. C. Zeng and D. Bertsimas, "Global flood prediction: A multimodal machine learning approach," in Proc. Workshop Tackling Climate Change with Mach. Learn., ICLR 2023, Jan. 2023, arXiv:2301.12548.

[10]. N. Karthikeyan et al., "Integrated disaster warning system for multi-hazard management," in Proc. ICEEI, 2025, pp. 1–7,doi: 10.1109/ICEEI68459.2025.11330341.

[11]. P. C. V. Chaganti et al., "Predicting landslides and floods with deep learning," in Proc. ICESC, 2023,pp.1259–1265,doi: 10.1109/ICESC57686.2023.10193456.

[12]. K. P. I. Karunawardhana et al., "Enhancing human safety through early detection of

floods and landslides in Sri Lanka," in Proc. ICITR,2024,pp.307–312,doi:10.1109/ICITR64794.2024.10857761.

[13]. M. Wahba et al., "Enhanced hazard mapping for flood and landslide risks using memetic programming and machine learning," IEEE Access, vol. 13, pp. 182410–182429,2025,doi:10.1109/ACCESS.2025.3623933.